Elastic Scattering Spectroscopy as a Diagnostic Tool for Apoptosis in Cell Cultures

Christine S. Mulvey, Allison L. Curtis, Satish K. Singh, and Irving J. Bigio

***Abstract*—Apoptosis, "programmed cell death," is a cellular process exhibiting distinct biochemical and morphological changes. There is much interest regarding the role of apoptosis in cancer and the response to cancer treatment. Although apoptosis can occur spontaneously in malignant tumors and often significantly retards their growth, the initial response to successful cancer treatment is often massive apoptosis. In typical *in vitro* studies, current apoptosis detection methods require cell culture disruption via fixation, trypsinization, and/or staining. Our aim is to develop a nondisruptive optical method of detecting and tracking apoptosis in living cells and tissues, initially focusing on cell cultures. Such a method would allow for real-time evaluation of apoptotic progression of the same cell culture over time without perturbation or alteration. We report initial studies on the use of *in vitro* elastic scattering spectroscopy (ESS) to monitor changes in light-scattering properties of cells due to apoptotic morphology changes. For a sequence of times post treatment, we have measured the angle-dependent scattering at a single wavelength and also the wavelength-dependent scattering at discrete angles, of treated and control cell cultures. A novel polar nephelometer, developed in our laboratory, was used to obtain the angle-dependent scattering for the range of 90–145°. Wavelength-dependent ESS measurements were made with a spectrometer, for several discrete near-forward angles. The results indicate that light scattering measurements can reliably discriminate between treated and control cells, correlating well with benchmark assays for apoptosis.**

***Index Terms*—Apoptosis, elastic scattering spectroscopy (ESS), noninvasive detection, nuclear morphology.**

I. Introduction

A. Apoptosis

APOPTOSIS is a normal, regulated cellular process often termed "programmed cell death," since the cell contains machinery that allows for its self-destruction. Apoptosis is responsible for the deletion of cells in normal tissues, and the death of cells due to pathological conditions. There is, perhaps, the most interest regarding the role of apoptosis in cancer. Apoptosis occurs spontaneously in malignant tumors and often significantly retards their growth [1]–[3]. It has also been clear for some time that apoptosis is enhanced by most cancer treatment modalities [4]. For all of these treatments, enhanced apoptosis is a desired response to treatment, and in fact, the initial response to current effective treatments is often massive apoptosis [3], [4].

Understanding of metabolic and morphological changes that occur during apoptosis provides opportunities to monitor apoptosis in tissue using noninvasive techniques, to provide diagnostic and prognostic information [5]. The earliest recognized morphological changes are nuclear. The nuclear chromatin condenses and segregates, forming well-defined, granular masses that are either collected along the inner surface of the nuclear membrane or are distributed as small masses throughout the nucleus. As condensation progresses, the nuclear membrane may become convoluted, and in most cases, the process progresses with the breaking up of the nucleus into discrete fragments where the segregation of the chromatin is maintained [1]–[3]. These fragments may show condensed chromatin occupying the whole surface, or they may have the chromatin forming crescent-shaped caps [1]. Starting coincidentally with these nuclear events, the cytoplasm progressively loses water resulting in a crowding of the organelles, each of which maintains its integrity, and the appearance of clear vacuoles. The cell membrane forms protuberances, which then separate, and the plasma membrane seals itself to form membrane-encompassed apoptotic bodies of roughly spherical shape. These bodies may or may not include nuclear fragments [1]–[3]. Apoptotic bodies are eliminated from the tissue through phagocytosis, in which the tissue cells are surrounded by phagocytes and digested by the engulfing cell's lysosomes [2]. With homeostatic apoptosis, there is no resulting inflammation or disruption of tissue architecture.

B. Current Detection Methods for Apoptosis

There exist several methods for detection of apoptosis *in vitro*, although detection can be challenging due to the dynamic nature of the apoptotic process. Apoptotic events can occur in as little as a few hours and may go undetected depending on sampling time [6], [7]. Current "gold-standard" methods include microscopy and flow cytometry, both of which require fixation and staining to exploit either the morphological or biochemical features of apoptosis. Microscopy allows for a qualitative observation of such changes in cell cultures, whereas flow cytometry can be used for quantifying the percentage of apoptotic cells in a sample. All current *in vitro* methods require either the addition of an exogenous agent during fixing or staining, and the physical/chemical disruption of the culture itself [8], [9].

Manuscript received September 6, 2007.

C. S. Mulvey is with the Department of Biomedical Engineering, Boston University, Boston, MA 02215 USA (e-mail: cmulvey@bu.edu).

A. L. Curtis was with the Department of Physics, University of Massachusetts, Boston, MA 02125 USA. She is now with the Molecular Imaging Group, Novartis Institute for Biomedical Research, Inc., Cambridge, MA 02139 USA (e-mail: ally26@gmail.com).

S. K. Singh is with the Department of Medicine, Boston University School of Medicine, Boston, MA 02118 USA (e-mail: satish.singh@bmc.org).

I. J. Bigio is with the Department of Biomedical Engineering and Electrical and Computer Engineering, Boston University, Boston, MA 02215 USA (e-mail: bigio@bu.edu).

Color versions of one or more of the figures in this paper are available online at http://ieeexplore.ieee.org.

Digital Object Identifier 10.1109/JSTQE.2007.910115

C. Elastic Scattering Spectroscopy

An ideal detection method would allow for the measurement of the state of a population of cells without perturbing the cells or altering their environment. That is, the measurement would be fast, and a tissue culture could be returned to the incubator following a measurement. In addition, it would be advantageous for a detection method to be sensitive to the apoptotic changes as early as possible. These two criteria would allow for more efficient testing of cell cultures in studies, for example, of anticancer and antiapoptosis agents. Such a method would also enable monitoring of a single population of cells over a time course, rather than requiring a new sample of cells at each time point, thereby allowing for a more accurate assessment of the cellular response.

With these criteria in mind, we are developing the use of elastic scattering spectroscopy (ESS) for apoptosis detection in cell cultures. The primary advantage of using ESS as a way to probe cell morphology is its inherent noninvasiveness. For cell cultures, fast measurements can be made (within seconds) with the cells in their native state, and they can then be returned to the incubator between measurement time points, allowing for a time course of measurements on the same culture sample. With proper analysis algorithms, cellular state can be determined in real time.

ESS is based on photons scattering elastically from cells, due to gradients and discontinuities in the refractive index. While cellular components are not perfectly spherical, the qualitative features of cellular scattering can be modeled using Mie theory. The most common model used for cells is the so-called coated sphere model, in which the cell is treated as two separate components: the scattering center and the surrounding cytoplasm. Since the coated sphere model is an application of Mie theory, the scatterers are modeled as homogeneous spheres [10]–[18]. The probability of scattering from a spherical particle illuminated by a plane wave is dependent on the "size parameter," $\alpha = 2\pi a n_m/\lambda$. The amount of scattering that occurs depends on multiple parameters including: the diameter of the scatterer (a), the index of refraction of the scatterer, the index of the surrounding medium (n_m), the illuminating wavelength (λ), and the scattering angle. By measuring the angle and/or wavelength dependence of scattering probability of cells, ESS can be used to infer information about the size and density of the structures responsible for scattering [10]. We expect that the differences in morphologies between normal and apoptotic populations of cells should produce detectable differences in scattering phase functions and spectra. Since pathologists often use microstructural features of cells and tissues for diagnosis, ESS can potentially be used as a diagnostic tool [10] for apoptosis.

II. Experiment Design

A. Instrument Design

Two different instruments were employed for measuring changes in elastic scattering from cells: 1) a polar nephelometer to measure the angular scattering distribution (the phase function) at discrete wavelengths and 2) a spectral system to measure the elastic scattering spectrum at discrete angles.

1) Nephelometer Design: Many ESS studies done on cells have employed the use of angular dependent measurements on cell suspensions with traditional goniometers. Measurements have been made on intact cells [10], [11], [14], [15], [19], [20] and on suspensions of isolated organelles [10], [11], [14], [20] in order to better understand organelle contributions to scattering. A number of groups have also managed to extract size distribution information of scatterers from angle-dependent measurements by fitting experimental data with various Mie fitting protocols [14], [20]. Most traditional goniometers employ laser illumination to a circular test space with a detector that rotates around the sample. A common drawback to these systems is lengthy testing times. With a fully actuated system, and angular measurement resolution of, say, 1°, a sweep of the full angular range takes several minutes [10], [15]. Systems that are not automated can require up to 30 min of testing time, depending on the intensity of the light source and the detector sensitivity. Furthermore, these systems tend to have limited angular resolution for shorter angle scan times [11].

A nephelometer, sometimes called a "turbidimeter," is a device for measuring suspended particulates with scattered light. Our group has previously designed a polar nephelometer for measuring the angle-dependent light-scattered intensity distribution of suspensions of particles, based on confocal imaging of the test space with off-axis parabolas [21], [22]. While the system was originally designed as a rapid particle sizer, in this study, we used it to measure the phase function of cells. A schematic of the polar nephelometer is shown in Fig. 1.

In the current version, a laser beam ($\lambda = 532\ \mathrm{nm}$, $P = 40\ \mathrm{mW}$) is linearly polarized and focused with a lens to the center of a cylindrical test space. A half-wave plate allows for rotation of the polarization to be either perpendicular or parallel to the scattering plane. The lens is chosen to produce a beam waist with diameter of about 100 μm. This ensures that a cell will be fully captured by the beam and will be far enough from the beam edge so that the illumination is approximately planar, allowing for comparison of experimental data with Mie theory calculations. The center of the test space is positioned at the focus of one of a pair of conjugated off-axis parabolas. Scattered light is collected by the parabola and refocused to the conjugate image of the test space by the second parabolic mirror. Each parabola has a scattered angular range of approximately 55°, but a greater angular range can be covered quickly by deflecting the laser beam to impinge on the test space from different angles. A rotating mirror, with the rotation axis at the second focus, sweeps out the angular range and passes the scattered light at each angle, through an aperture and a lens. Light collected through the aperture is split into parallel and perpendicular polarization states by a beamsplitting cube, and each polarization state is finally refocused by a second lens to an optical fiber and a photomultiplier.

The main advantage of this system is the speed at which measurements are taken. The rotating mirror samples the test space between 15 and 20 times per second. This ensures that the cells do not move in and out of the test space during the

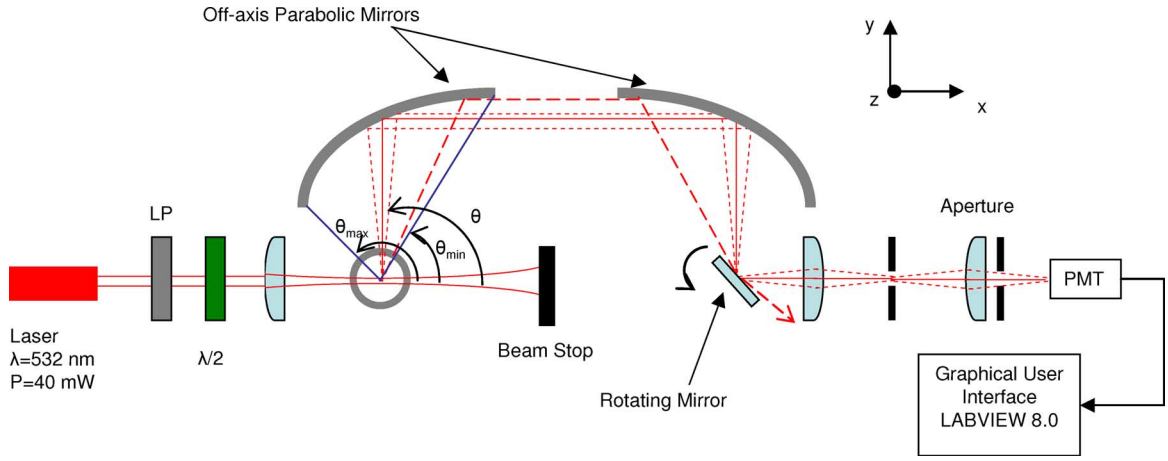

Fig. 1. Schematic of polar nephelometer.

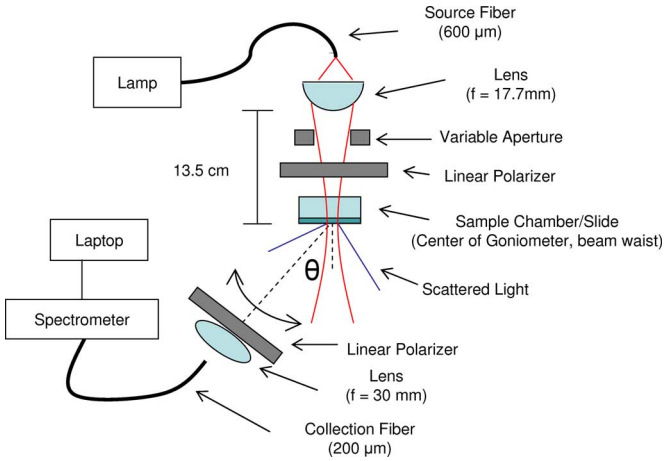

Fig. 2. Optical setup for ESS, spectral system.

measurement. This feature, combined with the narrow beam waist and an appropriate cell concentration, allows for the measurement of a single cell's phase function. If an average phase function is desired, multiple scans can be averaged to reduce noise, or single scans can be used to provide a size distribution of particles. The speed of measurements has other advantages. Short measurement times minimize the time that cells are out of the incubator, and also allows for good time resolution in time course measurements.

2) Spectral System Design: As the nucleus is a relatively large organelle and is significantly larger than the wavelength of the incident light, its size parameter is large, and scattering theory predicts that its contribution to cellular scattering should dominate in the forward direction [11], [23], [24]. In light of this observation, we have developed a system for measuring wavelength-dependent scattering from either suspensions or plated cell cultures in the near-forward direction. A schematic is shown in Fig. 2.

The optical setup consists of illumination and collection fibers, two lenses, two polarizers, and a glass-chamber culture slide to hold the sample. The output of the 600 μm illumination fiber (from a broadband halogen source) is imaged by a plano-convex lens ($f = 17.7$ mm) onto the test space, where light is approximately collimated. The lens is positioned to create a long Rayleigh range (this minimizes sensitivity to vertical placement of the sample), with the beam waist about 13.5 cm from the lens. A variable aperture is used to limit the intensity of light incident on the sample. When measurements are made, the aperture is open fully, and the diameter of the beam waist is approximately 3 mm. At some angles, scattering is dependent on polarization state, so two polarizers are used in the instrument: one to control the polarization incident on the sample, and the other to select the polarization viewed by the detector. The sample chamber is positioned such that the glass surface where the cells grow is at the beam waist. By placing the scatterers at the beam waist, the wavefront of the incident light is approximately planar, allowing for comparison with Mie theory modeling. This also allows for easy determination of scattering angle since the incident light is perpendicular to the plate. Paraxial scattered rays are linearly polarized and then collected by a thin lens ($f = 30$ mm) and passed through a 200 μm fiber to a spectrometer, with the collection fiber serving as an angle-limiting aperture. The thin lens, polarizer, and the collection fiber are rotated as a unit to measure spectra at different discrete scattering angles, using a stepper motor controlled with MATLAB, with an angular resolution of approximately 0.5°.

B. Data Collection and Analysis

1) Nephelometer: For each sample, two separate measurements are required. To achieve a good SNR, in these studies, a measurement typically consists of an average of 512 scans by the rotating mirror, requiring about 30 s. S- and P-polarization data are collected simultaneously. First, a measurement of the background level of scattering ($P_{\text{background}}$) is taken with only the culture growth medium in the sample tube, accounting for any scattering that takes place due to the medium, the sample tube, or any of the system's optical components. The second measurement (P_{sample}) is made of the cells suspended in the growth medium. The cells' phase function is calculated for each polarization using the following formula: $P_{\text{cells}} = P_{\text{sample}} - P_{\text{background}}$. To ensure that the resulting phase function does not depend on the intensity of the

illuminating light or the number of cells that passed through the sample volume during data collection, the resulting phase functions are normalized to the area under the curve.

2) Spectral System: For each sample and each angle of interest, six separate measurements of intensity as a function of wavelength are required. The first two measurements $(I_{\mathrm{spec.resp}})$ are made with the detector in line with the illumination (0° scattered angle) to capture the spectral characteristics of the system at polarization states parallel (P), and perpendicular (S), to the scattering plane. For the spectral response measurement, the setup includes all the components except the scattering particles. The aperture is partially closed to avoid saturating the detector. The measurement time is a few milliseconds. Next, background scattering measurements $(P_{\mathrm{background}})$ are made for both polarizations at each angle of interest with the aperture fully open, again including all components of the system except the particles or cells. This allows us to subtract any scattering from component surfaces or the growth medium itself. Finally, measurements (P_{sample}) are taken with the cells or particles at both polarizations at each angle of interest. The measurement time for both the background and cell measurements is a few seconds. To reduce noise, each measurement was first smoothed using a boxcar with a width corresponding to approximately $1\ \mathrm{nm}$. The scattering pattern for each polarization state is calculated by the following formula:

$$I_{\mathrm{particles/cells}} = \frac{I_{\mathrm{sample}} - I_{\mathrm{background}}}{I_{\mathrm{spec.resp.}}}.$$

To get a result that is not dependent on the number of particles in the illuminated sample space, we normalize the results to the area under the curve. Measurements were made for the spectral range 450–800 nm.

C. System Verification: Phantom Studies

The operation of the nephelometer was previously verified by comparison of experimentally collected phase functions from polystyrene spheres in water with Mie calculations [21], [22]. To verify the operation of the spectral system, measurements were also made on phantoms of polystyrene spheres $(n = 1.59)$ with known size distributions in water. To ensure that light collected was limited to mostly single-scattering events, suspensions were prepared such that the probability of a scattering event occurring as a photon passed through the sample was $\leq 10\%$. We collected scattering data from two phantoms, one with a mean diameter of 3.1 $\mu\mathrm{m}$, and the other with a mean diameter of 2.9 $\mu\mathrm{m}$. Both size distributions were assumed Gaussian with a variance of 5%, based on data provided by the manufacturer (Duke Scientific Corporation).

Fig. 3(a) shows experimental scattering at 11.9° from both the 2.9 and 3.1 $\mu\mathrm{m}$ particle suspensions. The experimental data are plotted using solid lines. Mie theory fitting was performed on the experimental data using a linear least-squares algorithm and the resulting fits are shown with dotted lines. Fig. 3(b) shows the size reconstructions from the least-squares algorithm. It should be noted that the fitted curves match well with the experimental data, and the resulting size distributions are consistent with the manufacturer's specifications for the particles. Fig. 3(c) shows experimental scattering collected from the 2.9 $\mu\mathrm{m}$ particle suspension at scattering angles of 11.9° and 14.9° along with the best Mie theory fits.

We note that, despite the small difference in mean particle size, and the overlap in size distribution, our system can readily discriminate between the two samples. These two plots taken together suggest that the system is capable of accurately observing scattering from particles and has a resolution of at least $200\ \mathrm{nm}$.

D. Apoptosis Induction

To investigate whether ESS can be sensitive to the changes in morphology that occur during apoptosis, we measured scattering from the samples of Chinese hamster ovary (CHO) cells, induced to undergo apoptosis, and compared them to the measurements from normally propagating cells. Using standard procedures, CHO cells were plated on polystyrene culture dishes and grown in Dulbecco's modification of Eagle's medium (DMEM) supplemented with 10% fetal bovine serum (FBS) and 1% penicillin and streptomycin (PAS). Atmosphere was held at 37 $^{\circ}\mathrm{C}$ and 5% $\mathrm{CO_2}$.

To induce apoptosis in CHO cells, they were incubated in DMEM supplemented with 2 $\mu\mathrm{M}$ staurosporine for periods up to 6 h. Since the staurosporine is carried in solution in dimethyl sulfoxide (DMSO), the same volume of DMSO was added to the control samples to compensate for any effects it might have on the cells. For initial verification that staurosporine induces apoptosis in CHO cells, an Annexin V-fluorescein isothiocynate (FITC) versus propidium iodide (PI) flow cytometry assay was performed on treated and control samples at various time points. The results of this assay $(n = 4)$ are shown in Fig. 4(a). The cells treated with staurosporine exhibit an increasing apoptotic population over time, with about 50% of the cells exhibiting apoptosis at 6 h, while the control cells have the same low percentage of apoptotic cells throughout the experiment.

While the flow cytometry assay gives a quantitative assessment of apoptosis using a biochemical membrane event, we are most interested in morphological changes in the cell. To assess nuclear morphology, we stained treated and untreated populations of cells with Hoechst 33342, which fluoresces blue when bound to DNA, at various time points from before treatment until 6 h after treatment. Nuclear condensation appears as brighter fluorescence. The resulting nuclear images are shown in Fig. 4(b)–(d). At the time of treatment [Fig. 4(b)], the staining is relatively uniform, indicating uncondensed DNA in the nuclei. The condensation of nuclear material becomes evident at 4 h [Fig. 4(c)] and is widespread by 6 h [Fig. 4(d)].

E. Cell Preparation for ESS Measurements

1) Nephelometer: To prepare for ESS measurements of the phase function, plated cultures of CHO cells were grown to confluence, then detached from the plate (trypsinized). If measurements were to take place within an hour of treatment, the cells were first trypsinized and resuspended in fresh DMEM. Once

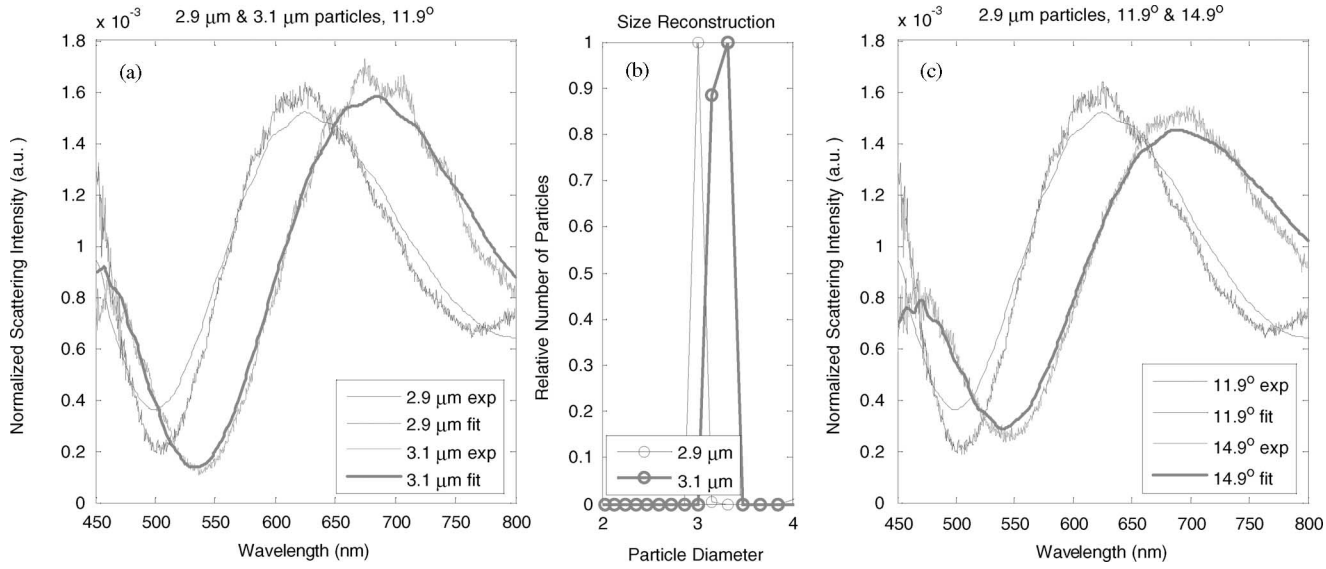

Fig. 3. Scattering from polystyrene sphere phantoms. (a) Comparison of experimental scattering with best fits to Mie theory for suspensions of $2.9\ \mu\mathrm{m}$ (thin line) and $3.1\ \mu\mathrm{m}$ (thick line) polystyrene spheres. (b) Reconstructed size distributions yielding the best fits to theory from the experimental data in (a). (c) Experimental scattering and the corresponding best fits for $2.9\ \mu\mathrm{m}$ particles at 11.9° and 14.9°.

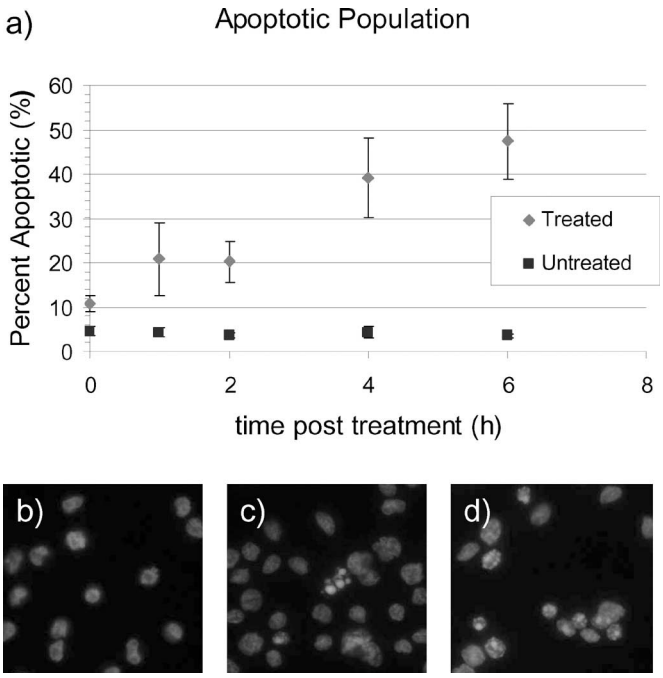

Fig. 4. Induction of apoptosis. (a) Apoptotic population assessed by AnnexinV-FITC flow cytometry. Fluorescence microscopy images (Hoechst 33342) of cell nuclei from cultures treated with staurosporine at various values of t. (b) $t = 0$ h. (c) $t = 4$ h. (d) $t = 6$ h.

transferred to the sample tube, either staurosporine in DMSO or a control volume of DMSO was added to a final concentration of $2\ \mu\mathrm{M}$. Scattering measurements were made beginning immediately after the treatment. Between measurements, the sample tubes were replaced in the incubator, and before each measurement, the tubes were inverted several times to keep the cells from settling. The same cell culture was measured for times up to an hour after the treatment. We wanted to minimize the time that the cells were in suspension, since it is not their native state; thus, for times later than 1 h posttreatment, we measured a new culture every half hour for times up to 6 h. These cultures were treated at the beginning of the experiment and were trypsinized and suspended in DMEM immediately preceding the measurements. Scattering was collected for the range of angles between 90° and 145° with subdegree resolution.

2) Spectral System: To prepare cells for scattering spectral measurements, they were plated on glass chamber slides and grown to confluence. The growth medium was aspirated and replaced with DMEM (without phenol red, which is normally used) already supplemented with either $2\ \mu\mathrm{M}$ staurosporine/DMSO or an equivalent volume of DMSO. Clear DMEM was used during ESS spectral measurements to avoid affecting the spectral shape. Scattering measurements were made on the cells at a scattering angle of 10.5° and the slides were returned to the incubator between measurements. Measurements were made on the same samples for time points up to 6 h.

III. Preliminary Cell Data and Discussion

A. Nephelometer Measurements

Scattering measurements were performed on five pairs of treated and untreated cell suspensions for times up to 1 h. For later measurement times (1–6 h), a new culture was required for each measurement. This experiment was repeated four times. In Fig. 5, we present the angular resolved scattering data from a single experiment at representative times to illustrate the changes in the cell suspension's phase function over time. The 0, 10, 20, and 40 min measurements were all preformed on the same cell suspension, and can thus, be easily compared. The 2 and 4 h measurements, however, each required a new sample, and therefore, a comparison to measurements at other times is more difficult to make. While data from only one trial are presented here, the phase functions measured in all trials showed the same trend over time.

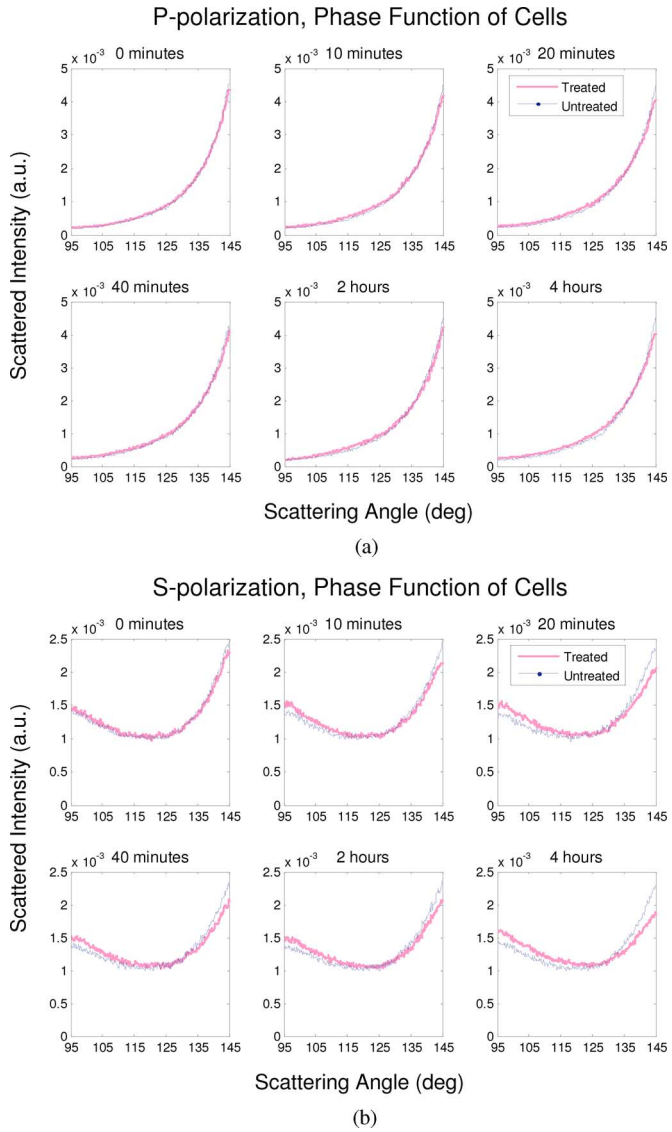

Fig. 5. Phase functions for treated and untreated suspensions of CHO cells for times posttreatment up to 4 h. (a) P-polarization. (b) S-polarization.

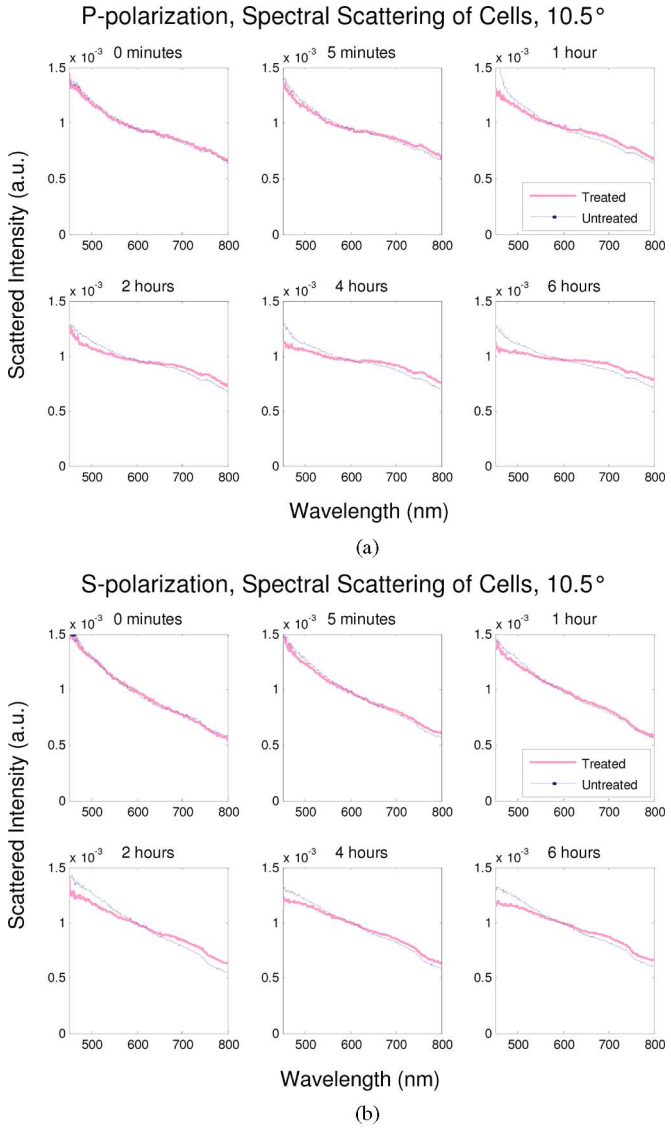

Fig. 6. Scattering from a single pair of cell cultures over time. (a) P-polarization. (b) S-polarization.

The first thing to note is that the cell suspension's phase function when using P-polarized light does not appear to vary significantly between treated and untreated samples at any time posttreatment [Fig. 5(a)]. The phase function, when measured in S-polarization [Fig. 5(b)], however, does show a clear difference between treated and untreated samples at later time points. It is encouraging that there is little difference between the phase functions immediately after the treatment, and that the difference appears to progress for the first 20 min. It is rather unexpected, however, that the difference in phase function appears so early, beginning at 10 min, and does not change much after 20 min. Given the short time scale, it is unlikely that the observed difference in phase function is due to a change in the cells' nuclear morphology, as this is not observable by microscopy until some time later.

We do believe, however, that the change in scattering is likely due to a cellular event and not simply due to the addition of staurosporine, since there is no significant difference immediately after adding staurosporine and DMSO to one sample compared with adding only DMSO to the other. Furthermore, a difference still exists between samples at later time points, for which the cells are treated while still on plates, but with the chemicals being removed when the cells are suspended in fresh medium before measurement. We also note that the resuspension of plated cell cultures is not ideal for ESS measurements, since it is unclear what effects disrupting the cells from their native state may have on cellular morphology. Despite this drawback in preparation, however, the fact that a difference in phase function is observable between treated and control samples, and perhaps, more importantly, that the progression in phase function over time has been reproducible in each trial, is encouraging in developing ESS as a tool for monitoring apoptosis.

B. Spectral System Measurements

For these measurements, cells remain plated on their culture plates, and we avoid the disruptive process of trypsinizing and

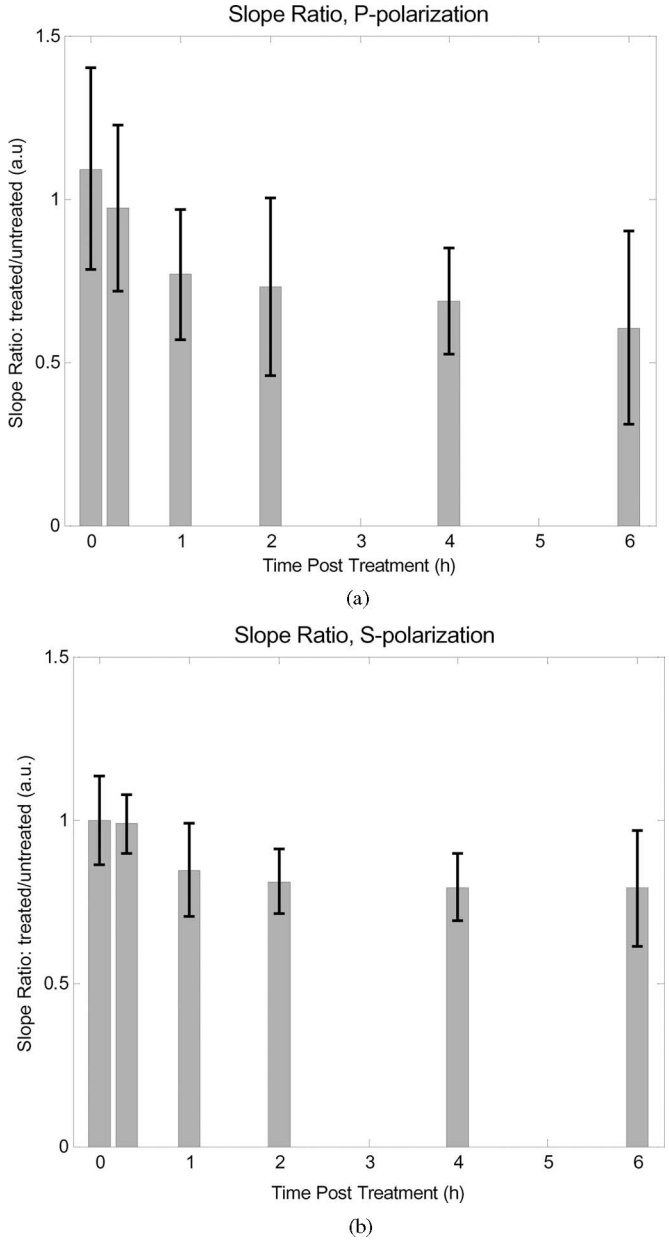

Fig. 7. Average ratio of the slopes of the treated and control cells at each time point. (a) P-polarization. (b) S-polarization.

suspending the cells. Fig. 6 shows scattering spectral data from one representative pair of cell culture plates, one treated with staurosporine/DMSO, the other treated with a control volume of DMSO, measured over a period of 6 h using P- [Fig. 6(a)] and S-polarization [Fig. 6(b)]. We note that in the near forward direction, the scattering is very similar for both polarization states, and thus, the two figures show similar spectra. Immediately following treatment, the treated and untreated spectra overlap and show only a slight change. At subsequent time points, the two spectra become increasingly separate, suggesting a progressing cellular process. This trend has proven repeatable over a large number of samples $(n = 18)$.

It should be noted, however, that there is some variability in the shapes of the spectra from sample to sample. In order to illustrate this variability, we have calculated the slope for each data set between 550 and 650 nm, and taken the ratio of the slopes of each pair of treated and untreated samples. The mean and standard deviation of these ratios were taken for each time point in both S- and P-polarizations. These data are shown in Fig. 7(a) and (b). Again, it is encouraging that at very early time points, the ratio is centered close to 1, indicating that there is little difference in the shape of the spectra. As time progresses, the ratio deviates farther from 1, indicating that the spectra diverge. It is unclear at this time whether the variability in signal is due to biological variation or due to experimental artifact, but the statistically strong and repeatable trend is promising for the use of ESS as a method to monitor apoptosis.

IV. Conclusion

We are currently investigating the source of variations shown in Fig. 7, and an effort must be made to understand the differences in the scattering signal. A necessary step in developing ESS as a diagnostic tool for the detection of apoptosis is to relate the morphological features of the organelles to the bulk optical properties measured by understanding how light scatters from structures within the cells [10], [11], [19], [25].

While treatment of the nucleus as a Mie scatterer implies that much of the scattered light is in the forward direction because the size parameter is large, there is also an appreciable amount of backscatter [12]. Backman *et al*. have noted that the scattering cross section of nuclei exhibit a periodicity with wavelength that introduces a fine structure to backscattered reflectance [26]. Different groups have extracted size information with various types of Mie fitting. [12], [13] While these studies suggest that measurements of backscatter can extract nuclear size, it is important to note that cell nuclei may not behave like homogeneous Mie scatterers. Richards-Kortum *et al*. have illustrated that Mie modeling for extraction of nuclear size may be appropriate for forward scattering, but the fine detail of nuclear morphology will have an effect on backscatter [19], [24], [25]. In the case of apoptosis, this is likely to be especially true, since the nucleus fragments into multiple smaller structures.

For a future publication, we plan to modify the spectral system to allow for backscattering measurements. Furthermore, if backscattering measurements prove to be sensitive to apoptosis, the use of a tissue-probe design would be suitable for applications *in vivo*. We are also in the process of modifying the existing nephelometer to allow for phase function measurements on plated cells.

Acknowledgment

The authors thank Dr. S. Krishnan for the CHO cells and for patiently sharing her knowledge of cell biology and cell culture techniques.

References

[1] A. H. Wylie, J. F. R. Kerr, and A. R. Currie, "Cell death: The significance of apoptosis," *Int. Rev. Cytol*., vol. 68, pp. 251–306, 1980.

[2] J. F. R. Kerr, J. Searle, B. V. Harmon, and C. J. Bishop, "Apoptosis," in *Perspectives on Mammalian Cell Death*, C. S. Potten, Ed. Oxford, U.K.: Oxford Univ. Press, 1987, pp. 93–128.

[3] J. F. R. Kerr, C. M. Winterford, and B. V. Harmon, "Apoptosis—Its significance in cancer and cancer therapy," *Cancer*, vol. 73, pp. 2013–2026, Apr. 1994.
[4] S. W. Lowe and A. W. Lin, "Apoptosis in cancer," *Carcinogenesis*, vol. 21, pp. 485–495, Mar. 2000.
[5] M. Brauer, "In vivo monitoring of apoptosis," *Prog. Neuro-Psychopharmacol. Biol. Psychiatry*, vol. 27, pp. 323–331, Apr. 2003.
[6] P. J. M. Best, D. Hasdai, G. Sangiorgi, R. S. Schwartz, D. R. Holmes, Jr., R. D. Simari, and A. Lerman, "Apoptosis: Basic concepts and implications in coronary artery disease," *Arterioscler. Thromb. Vasc. Biol.*, vol. 19, pp. 14–22, Jan. 1999.
[7] A. Saraste and K. Pulkki, "Morphologic and biochemical hallmarks of apoptosis," *Cardiovasc. Res.*, vol. 45, pp. 528–537, Feb. 2000.
[8] M. C. Willingham, "Cytochemical methods for the detection of apoptosis," *J. Histochem. Cytochem.*, vol. 47, pp. 1101–1109, Sep. 1999.
[9] R. Sgonc and J. Gruber, "Apoptosis detection: An overview," *Exp. Gerontol.*, vol. 33, pp. 525–533, Sep. 1998.
[10] J. R. Mourant, M. Canpolat, C. Brocker, O. Esponda-Ramos, T. M. Johnson, A. Matanock, K. Stetter, and J. P. Freyer, "Light scattering from cells: The contribution of the nucleus and the effects of proliferative status," *J. Biomed. Opt.*, vol. 5, pp. 131–137, Apr. 2000.
[11] J. R. Mourant, J. P. Freyer, A. H. Hielscher, A. A. Eick, D. Shen, and T. M. Johnson, "Mechanisms of light scattering from biological cells relevant to noninvasive optical-tissue diagnostics," *Appl. Opt.*, vol. 37, pp. 3586–3593, Jun. 1998.
[12] V. Backman, R. Gurjar, K. Badizadegan, I. Itzkan, R. R. Dasari, L. T. Perelman, and M. S. Feld, "Polarized light scattering spectroscopy for quantitative measurement of epithelial cellular structures in situ," *IEEE J. Sel. Topics Quantum Electron.*, vol. 5, no. 4, pp. 1019–1026, Jul./Aug. 1999.
[13] K. Sokolov, R. Drezek, K. Gossage, and R. Richards-Kortum, "Reflective spectroscopy with polarized light: Is it sensitive to nuclear morphology?," *Opt. Express*, vol. 5, pp. 302–317, Dec. 1999.
[14] J. R. Mourant, T. M. Johnson, S. Carpenter, A. Guerra, T. Aida, and J. P. Freyer, "Polarized angular dependent spectroscopy of epithelial cells and epithelial cell nuclei to determine the size scale of scattering structures," *J. Biomed. Opt.*, vol. 7, pp. 378–387, Jul. 2002.
[15] A. Brunsting and P. F. Mullaney, "Differential light scattering from spherical mammalian cells," *Biophys. J.*, vol. 14, pp. 439–453, Jun. 1974.
[16] H. Fang, M. Ollero, E. Vitkin, L. M. Kimerer, P. B. Cipolloni, M. M. Zaman, S. D. Freedman, I. J. Bigio, I. Itzkan, E. B. Hanlon, and L. T. Perelman, "Noninvasive sizing of subcellular organelles with light scattering spectroscopy," *IEEE J. Sel. Topics Quantum Electron.*, vol. 9, no. 2, pp. 267–276, Mar./Apr. 2003.
[17] J. D. Wilson and T. H. Foster, "Mie theory interpretations of light scattering from intact cells," *Opt. Lett.*, vol. 30, pp. 2442–2444, Sep. 2005.
[18] N. N. Boustany, S. C. Kuo, and N. V. Thakor, "Optical scatter imaging: Subcellular morphometry in situ with Fourier filtering," *Opt. Lett.*, vol. 26, pp. 1063–1065, Jul. 2001.
[19] R. Drezek, A. Dunn, and R. Richards-Kortum, "Light scattering from cells: Finite-difference time-domain simulations and goniometric measurements," *Appl. Opt.*, vol. 38, pp. 3651–3661, Jun. 1999.
[20] J. D. Wilson, C. E. Bigelow, D. J. Calkins, and T. H. Foster, "Light scattering from intact cells reports oxidative-stress-induced mitochondrial swelling," *Biophys. J.*, vol. 88, pp. 2929–2938, Apr. 2005.
[21] J.-L. Castagner and I. J. Bigio, "Polar nephelometer based on a rotational confocal imaging setup," *Appl. Opt.*, vol. 45, pp. 2232–2239, Apr. 2006.
[22] J.-L. Castagner and I. J. Bigio, "Particle sizing with a fast polar nephelometer," *Appl. Opt.*, vol. 46, pp. 527–532, Feb. 2007.
[23] V. Backman, V. Gopal, M. Kalashnikov, K. Badizadegan, R. Gurjar, A. Wax, I. Georgakoudi, M. Mueller, C. W. Boone, R. R. Dasari, and M. S. Feld, "Measuring cellular structure at submicrometer scale with light scattering spectroscopy," *IEEE J. Sel. Topics Quantum Electron.*, vol. 7, no. 6, pp. 887–893, Nov./Dec. 2001.
[24] A. Dunn, C. Smithpeter, A. J. Welch, and R. Richards-Kortum, "Finite-difference time-domain simulation of light scattering from single cells," *J. Biomed. Opt.*, vol. 2, pp. 262–266, Jul. 1997.
[25] R. Drezek, A. Dunn, and R. Richards-Kortum, "Light scattering from cervical cells throughout neoplastic progression: Influence of nuclear morphology, DNA content, and chromatin texture," *J. Biomed. Opt.*, vol. 8, pp. 7–16, Jun. 2003.
[26] L. T. Perelman, V. Backman, M. Allace, G. Zonios, R. Manoharan, A. Nusrat, S. Shields, M. Seiler, C. Lima, T. Hamano, I. Itzkan, J. Van Dam, J. M. Crawford, and M. S. Feld, "Observation of periodic fine structure in reflectance from biological tissue: A new technique for measuring size distribution," *Phys. Rev. Lett.*, vol. 80, pp. 627–630, Jan. 1998.

Christine S. Mulvey received the B.S. degree in engineering sciences from Harvard College, Cambridge, MA, in 2004. She is currently working toward the Ph.D. degree in biomedical engineering at the Biomedical Optics Laboratory, Boston University, Boston, MA.

Her current research interests include noninvasive diagnostics with emphasis on detection and tracking of apoptosis in cell cultures.

Allison L. Curtis received the B.S. degree in physics from the McGill University, Montreal, QC, Canada, in 2004 and the M.S. degree in applied physics from the University of Massachusetts, Boston, in 2007.

She is currently a Research Associate in the Molecular Imaging Group, Novartis Institute for Biomedical Research, Inc., Cambridge, MA. As part of her graduate program, she completed an internship in Dr. Irving Bigio's Biomedical Optics Laboratory, Boston University, Boston. Her current research interests include wavelength-dependent optical detection of apoptosis.

Satish K. Singh received the B.A. (*summa cum laude*) and M.D. degrees in medical sciences from Boston University, Boston, MA.

He is currently an Assistant Professor of Medicine at Boston University School of Medicine and Staff Gastroenterologist, Boston Medical Center, and VA Boston Healthcare System, Boston, MA. Following internship and residency in internal medicine at Strong Memorial Hospital of the University of Rochester, Rochester, NY, he pursued clinical and research fellowships in gastroenterology and cellular and molecular physiology at Yale University, New Haven, CT, where he joined the faculty until his recruitment to Boston University in 2001. He is an experienced live-cell Microscopist and is the Founding Director of the Perkin-Elmer Center for Cell Imaging in the Evans Department of Medicine, Boston University School of Medicine. His current research interests include diarrheal and colonic diseases with a more recent translational focus on the design, engineering, and clinical validation of spectroscopic methods for gastrointestinal endoscopy.

Irving J. Bigio received the Ph.D. degree in physics from the University of Michigan, Ann Arbor, in 1974.

From 1974 to 2000, he was a scientific Staff Member, at Los Alamos National Laboratory, where he was also the Leader of the Laser Science and Applications Program (1988–1994). He has been a Fulbright Senior Scholar at the Weizmann Institute of Science, in Israel, a Visiting Professor at the University of Copenhagen, Copenhagen, Denmark and a Guest Fellow of Pembroke College at the University of Oxford, Oxford, U.K. Since February 2001, he has been at the Boston University, where he is currently a Professor in the Departments of Biomedical Engineering, Electrical and Computer Engineering, and Physics. He holds several patents for biomedical optics instrumentation. He serves on several government advisory panels and on external advisory boards for companies and academic institutions. He is currently leading a multiinstitutional program under the NIH/NCI Network for Translational Research in Optical Imaging, comprising several medical research centers in the United States and Europe.

Dr. Bigio was the recipient of three R&D-100 Awards for the development of biomedical optical devices. He is a Fellow of the Optical Society of America and the American Institute of Medical and Biological Engineering, and is a Member of the American Physical Society and the Society of Photonic and Instrumentation Engineers (SPIE).